NATIONAL RADIO ASTRONOMY OBSERVATORY
Green Bank, West Virginia

Electronics Division Internal Report No. 16

THE MEASUREMENT OF THE DIAMETERS OF RADIO SOURCES WITH PENCIL BEAM ANTENNAS

P. Mezger and P. Stumpff

AUGUST 1963

NUMBER OF COPIES: 75

THE MEASUREMENT OF THE DIAMETERS OF RADIO SOURCES WITH PENCIL BEAM ANTENNAS

P. Mezger and P. Stumpff

1. Introduction

For the measurement of the characteristics of pencil beam antennas by means of radio sources it is very important to know the size of these radio sources. Let $f_m = \exp\left\{-\xi^2 (0.6/\Theta_E)^2 - \eta^2 (0.6/\Theta_H)^2\right\}$ be the main beam pattern of the antenna, $T = T_o \psi(\xi, \eta)$, $\psi\ (0, 0) = 1$ the distribution of the brightness temperature of the radio source. The antenna temperature is measured while the source drifts through the antenna beam, and is related to the brightness temperature distribution by the antenna convolution integral

$$(1) \qquad T_A(\xi, \eta) = T_o \frac{1 - \beta_m}{\Omega_m} \int_{-\infty}^{+\infty} \int d\xi' d\eta' f_m(\xi - \xi', \eta - \eta') \psi(\xi', \eta')$$

This integral has been evaluated for various distribution functions [1]. As long as the half width angular diameters of the sources are smaller than the beamwidth of the antenna, the resulting curves do not depend much on the distribution function and the assumption of a gaussian distribution function represents a fairly good approximation for any real radio source. Then, the half power beamwidth (HPBW) Θ'_A of the observed drift curve is related to the HPBW of the antenna, Θ_A, and the source, Θ_S, respectively, by

$$(2) \qquad \Theta'_A = \sqrt{\Theta_A^2 + \Theta_S^2}$$

With the same assumption the relation between antenna temperature T_A and flux density S_ν becomes

$$(3) \qquad S_\nu = \frac{2kT_A}{A} \left(1 + \frac{\Theta_S^2}{\Theta_A^2}\right)$$

To show the importance of these relations for antenna measurements, let us take as an example the 85-foot antenna at 4 cm wavelength, whose effective area and HPBW shall be determined by using Cas A with an angular diameter of about 3'. With a HPBW of

the antenna of 6.3', equation (2) leads to a correction of 11% for the HPBW and equation (3) to a correction of 23% for the effective antenna area. The same correction factor holds, of course, if the flux density of a radio source shall be determined from the measured antenna temperature. This is the reason that observations of the flux densities of the strongest radio sources, made recently at 10 GHz with an 85-foot telescope, have not been published, since it was not clear which correction factor should be used.

Edward Ng, a NRAO summer student, compiled the results of all measurements of the brightness distribution of the strongest radio sources. Figures 1a and 1b show the measured source diameters of Tau A in EW and NS direction, respectively. The assumption of a gaussian distribution of the brightness temperature seems to be justified. The measurements between 1 and 10 GHz are consistent, whereas the results obtained at higher and lower frequencies show relatively large dispersion.

All measured diameters of Cas A lay between 3' and 4' in NS as well as in EW direction (with the exception of pencil beam measurements as may be seen in Figure 2). All observers agree that the brightness temperature distribution of Cas A is very near to an uniformly radiating disk.

The measured diameters of Orion show a very large dispersion (Figure 3). The true value lies probably somewhere between 3.5' and 5'. A gaussian distribution seems to be justified.

Cyg A is well known to be a multiple source, with the two sources spaced about 100" near EW. In NS Cyg A is a very narrow source.

The numbers in Figures 1 through 3 are related to the literature references by Table 1.

TABLE 1

RESULTS OF ANGULAR SIZE OF TAU A AT VARIOUS FREQUENCIES

No.	ν Mc/s	β'_{EW}	β'_{NS}	Method of observing	Year publ.	Reference
1.	38	6.0'	---	Occultation	1956	Costain, et al, MN 116, 380
2.	81	2.5'	---	Occultation	1956	Costain, et al, MN 116, 380
3.	86	8.5'	8.5'	Occultation	1958	Udaltsov, et al, Soviet Ast. 2
4.	101	4.3'	4.2'	Interferometer	1953	Mills, Aust. J. Phys., 6, 452
5.	214	5.0' $\pm$ 0.6'	---	Interferometer	1954	Baldwin, Observatory 74, 120
6.	400	3.5'	---	Occultation	1957	Seeger & Westerhout, BAN, 13, 313
7.	960	3.3' $\pm$ 0.4'	3.7' $\pm$ 0.4'	Interferometer	1962	Maltby & Moffet, Ap. J., Suppl. 7, 93
8.	1420	3.2'	2.9'	Interferometer	1962	Lequeux, Ann. d'As., 25, 221
9.	1420	3.5'	3.5'	Christensen Cross	1962	Twiss, et al, Aust. J. Phys., 15, 378
10.	2700	<1.5'	<1.5'	Pencil Beam	1960	Altenhoff, et al, U. of Bonn, Pub. No. 59
11.	2930	Not resolved	---	Pencil Beam	1960	Sloanaker & Nichols, AJ, 65, 109
12.	3300	3.3'	3.9'	Fan Beam	1963	Little, Ap. J., 137, 164
13.	9400	3.4'	---	Pencil Beam	1961	Karachun, et al, Soviet Ast. 5, 59
14.	9400	3.5'	---	Fan Beam	1960	Pariiskii, Izv. GAO Pulkova, 21, 45
15.	10,000	3.4' $\pm$ 0.1'	>6.0'	Fan Beam	1959	Apushkinskii, et al, Soviet Ast., 3, 717
16.	16,700	4.1' $\pm$ 0.5'	3.4' $\pm$ 0.5'	Pencil Beam	1961	Barrett, Ap. J., 134, 945
17.	37,500	4.5'	---	Pencil Beam	1961	Kuzmin, et al, Doklady, 140, 81

β'_{EW} - angular size in east-west in min. of arc.

β'_{NS} - angular size in north-south in min. of arc.

Note. Boishot, et al did occultation measurement also, at 170 Mc/s. No explicit results are given. Little estimated the source to be 3.5' x 2.5'. See Boishot, et al (1956), C.R. 242, 1849 and Little (1963), Ap. J., 137, 171.

TABLE 2

RESULTS OF ANGULAR SIZE OF CAS A AT VARIOUS FREQUENCIES

No.	ν Mc/s	β'_{EW}	β'_{NS}	Method of observing	Year publ.	Reference
1.	127	4'	---	Interferometer	1959	Jennison & Latham, MN 119, 174
2.	960	>3.5'	3.8' ± 0.5'	Interferometer	1962	Maltby & Moffett, Ap. J., Suppl. 7, 93
3.	1420	4.0'	4.0'	Interferometer	1962	Lequeux, Ann. d'As. 25, 221
4.	2700	<1.5'	---	Pencil Beam	1960	Altenhoff, et al, U. of Bonn, Pub. 59
5.	2800	3' - 4'	3' - 4'	Interferometer	1959	Rowson, MN 119, 26
6.	2930	Not resolved	Not resolved	Pencil Beam	1960	Sloanaker & Nichols, AJ 65, 109
7.	9400	4'	4'	Pencil Beam	1961	Karachun, et al, Soviet Ast. 5, 59
8.	16,700	3.7' ± 0.5'	3.8' ± 0.5'	Pencil Beam	1961	Barrett, Ap. J. 134, 945

β'_{EW} - angular size in east-west in min. of arc.

β'_{NS} - angular size in north-south in min. of arc.

TABLE 3

RESULTS OF ANGULAR SIZE OF ORION NEBULA AT VARIOUS FREQUENCIES

No.	ν Mc/s	β'_{EW}	β'_{NS}	Method of observing	Year publ.	Reference
1.	960	$4.1' \pm 0.4'$	$4.8' \pm 0.4'$	Interferometer	1962	Maltby & Moffett, Ap. J., Suppl. 7, 93
2.	1420	$3'$	---	Christensen Cross	1960	Twiss, et al, Observatory 80, 153
3.	1420	$4'$	---	Interferometer	1962	Lequeux, Ann. d'As. 25, 221
4.	2700	$5'$	$5'$	Pencil Beam	1960	Altenhoff, et al, U. of Bonn, Pub. No. 59
5.	2930	$7' \pm 0.5'$	$7' \pm 1.0'$	Pencil Beam	1960	Sloanaker & Nichols, AJ 65, 109
6.	3300	$3.5'$	---	Fan Beam	1963	Little, Ap. J. 137, 164
7.	3600	$2.2'$	$2.2'$	Fan Beam	1960	Pariiskii, Soviet Ast. 5, 611
8.	8000	$3.2'$	---	Pencil Beam	1961	Menon, NRAO Pub. No. 1
9.	9400	$5.1' \pm 0.5'$	$5.1' \pm 0.5'$	Pencil Beam	1961	Karachun, et al, Soviet Ast. 5, 59
10.	16,700	$4.0' \pm 0.7'$	$4.1' \pm 0.7'$	Pencil Beam	1961	Barrett, Ap. J. 134, 955

β'_{EW} - angular size in east-west in min. of arc.

β'_{NS} - angular size in north-south in min. of arc.

2. Experimental Results

The experimental results described in the following have been obtained with a total power double channel superheterodyne receiver, whose local oscillator has been tuned to the frequency 7.6 GHz. The measurements at this frequency are part of a series of antenna measurements at various frequencies between 1.4 and 8 GHz, which aim to relate the high frequency performance of the 85-foot antenna to the mechanical accuracy of the reflector. The resulting characteristics of the 85-foot antenna at 7.6 GHz are given in Appendix I. In this section we give only the results of various drift and scan measurements in EW and NS direction of the radio sources Cas A, Cyg A, Tau A, and Orion. The observations were made on July 21 and 22. The sky was cloudy on July 21 and partially cloudy on July 22. So it is reasonable that the quality of the records taken on July 22 is better.

Records of very bad quality have been omitted, and the remaining records were weighted according to quality. A mean curve has been drawn to fit the actual record as well as possible. Then the curves have been tabulated at one minute intervals and these values have been normalized to the maximum value. Since the maximum antenna temperature T_A (Cas A) = 33 °K is very small as compared to the noise temperature of the receiver ($\approx$ 2000 °K), no correction for the detector law is needed. The results obtained for each individual drift or scan curve have been plotted on transparent paper. By superimposing the transparent plots of one series of measurements so as to get the smallest possible dispersion in the middle and upper part of the curves, a resulting mean curve has been obtained.

Figures 4 through 6 show three typical resulting plots classified as "good" and "bad", respectively. The curves drawn in these figures are the gaussian curves which fit best the measured points in the half power region.

The apparent HPBW's of the 85-foot antenna obtained with four radio sources as mean values of a set of individual records are compiled in Table 4.

TABLE 4

Radio source	Date of measurement	Extreme values for the measured HPBW		HPBW for the best fitting gaussian approximation	
		α	δ	α	δ
Cas A	7-21-63 7-22-63	6.95' - 7.10' 6.85' - 7.15'	6.5' - 6.6' 6.8' - 6.8'	7.0' 6.95'	6.5' 6.8'
Cyg A	7-21-63 7-22-63	6.6' - 6.95' 6.7' - 6.92'	6.3' - 6.4' 6.2' - 6.6'	6.6' 6.8'	6.3' 6.35'
Orion	7-22-63	7.25' - 7.4'	7.1' - 7.6'	7.3'	7.4'
Tau A	7-22-63	6.9' - 7.0'	6.8' - (7.2')	6.95'	6.8'

A detailed discussion of the individual sets of measured curves leads to the following apparent HPBW's.

TABLE 5

Radio source	α	δ
Cyg A	6.7' ± 0.1'	6.3' ± 0.1'
Cas A	7.0' ± 0.1'	6.8' ± 0.0'
Tau A	7.0' ± 0.1'	6.8' ± 0.2'
Orion	7.3' ± 0.1'	7.4' ± 0.2'

As is known from interferometer measurements, Cyg A is a very narrow radio source in the NS direction. We believe that HPBW measured in declination with Cyg A represents the true beamwidth of the antenna. C. M. Wade's semi-empirical formula for the beamwidth of a normally tapered feed is

$$\frac{\Theta_A}{\text{min. of arc}} = 4.176 \cdot 10^3 \frac{\lambda}{D} \tag{4}$$

which leads for 7.6 GHz, to a beamwidth of the 85-foot antenna of 6.37'. Our measurements with a similar horn feed at 1420 MHz have shown that the main beam of the antenna has very nearly a circular cross-section. The assumption of a circular main beam with a HPBW of 6.3' seems to be justified. We therefore start the evaluation of the HPBW of the four radio sources from the measured apparent antenna HPBW Θ_A' compiled in Table 2 and with $\Theta_A = 6.3'$ by means of equation (2).

TABLE 6

Radio source	Source diameters in α	Source diameters in δ
Cyg A	2.38' ± 0.4'	0' ± 0.1'
Cas A	3.05' ± 0.3'	2.6' ± 0.0'
Tau A	3.05' ± 0.3'	2.6' ± 0.7'
Orion	3.68' ± 0.3'	3.88' ± 0.5'

3. Discussion of the Results

The values of Table 3 have been inserted in the diagrams (Figures 1 through 3). Our results are consistent with the majority of other measurements which have been obtained with interferometers. But they all lie at the lower limit of those previous measurements.

The accuracy of our measurements could be considerably improved by using a switched receiver with a lower noise temperature as well as by using a recorder with a larger scale. It seems interesting, and worthwhile, to repeat these measurements, perhaps at a slightly higher frequency (≈ 8 GHz). Also, we propose to make similar measurements with the 85-foot telescope at 5 GHz (MASER) and with the 300-foot telescope at 1420 MHz. In both cases, the larger HPBW of the antennas (≈ 10') would be compensated by the higher sensitivity (MASER) or the higher antenna temperature (300-foot telescope).

The main problem in measuring source diameters with pencil beam antennas remains the determination of the true antenna HPBW. In the case of the 85-foot telescope declination scans with Cyg could be used. In Appendix II the possibility is discussed of using the edge of the moon for the determination of the true antenna HPBW.

In the case of the 300-foot telescope it seems possible to take a true point source for the HPBW measurement. For example, a rough check has shown the following values for the apparent HPBW of the 300-foot telescope at 1420 MHz.

TABLE 7

	Virgo A	Tau A
Apparent HPBW	9.52'	10.52'

Assuming that Virgo A represents a true point source at 1420 MHz we find the source diameter of Tau A by using equation (2), which gives the value of 4.8'. Since the values in Table 7 are single observations the accuracy of these single values is poor, but it shows that the effect of beam broadening seems to be large enough to give accurate results, if sufficient observations are taken.

APPENDIX I

THE CHARACTERISTICS OF THE 85-FOOT ANTENNA AT 7.6 GHz

The antenna temperature of Cas A at 7.6 GHz has been measured

(5) $$T_A = 33\ ^\circ K \pm 5\ ^\circ K$$

With $S_{7.6\ GHz}$ (Cas A) $= 6.5 \cdot 10^{-24}$ W m^{2}Hz and $\Theta_S = \sqrt{3.05 \times 2.6} = 2.8'$, equation (3) gives

(6) $$A = \frac{2kT_A}{S_\nu} \left(1 + \frac{\Theta_S^2}{\Theta_A^2}\right) = 168\ m^2 \pm 16\%$$

The antenna efficiency becomes $\eta = 32\%$, the main beam solid angle $\Omega_m = 1.2 \cdot 10^{-2}$ deg^2, and the antenna solid angle $\Omega = 3.1 \cdot 10^{-2}$ deg^2. With these solid angles the main beam stray factor $\beta_m = 0.61$ has been evaluated.

It was not possible to measure the zenith antenna temperature and hence to calculate the stray factor β_{II}.

APPENDIX II

DETERMINATION OF THE ANTENNA HPBW OF A CONVOLUTION WITH THE LIMB OF THE MOON

At high frequencies it becomes very difficult to determine the true HPBW of a large antenna, partly because the HPBW is of the same order as the size of the strongest sources, and partly because the flux density of the radio sources is weak at those frequencies. The moon is then one of the brightest radio sources. Because of the lack of an atmosphere the transition between the surface temperature of the moon ($\approx$ 230 °K) and the background temperature is very sharply defined. This is the reason that we investigate the possibility of determining the antenna main beam from a drift curve over the moon's dish.

The mathematical representation of the antenna convolution integral is given in equation (1). Let us now assume a constant brightness temperature over the disk of the moon

$$T = \begin{cases} T_M & \text{within the disk of the moon} \\ 0 & \text{elsewhere} \end{cases} \tag{7}$$

Let us further assume a gaussian shaped main beam with different HPBW, Θ_E and Θ_H in the two principal planes of the antenna. Generally the antenna feeds are mounted so that the principal planes coincide with the EW and NS directions, respectively This assumption simplified the following calculation considerably without being a severe limitation on the proposed measuring method.

Starting from equation (1), we calculate the drift curve for the moon passing through the antenna so that at one moment the center of the moon's disk coincides with the electrical axis of the antenna. Further, it is assumed that the electrical (ζ -) plane of the antenna is oriented EW. With equation (7) inserted in equation (1) one obtains

$$T_A(x, o) = 2T_M \frac{1 - \beta_m}{\Omega_m} \int_{\zeta' = \eta' = 0}^{2R} \int^{\eta_L'(\zeta)} e^{-a^2(\zeta' + x)^2} e^{-b^2\eta'^2} d\eta' d\zeta' \tag{8}$$

The corresponding geometry may be seen in Figure 7. Equation (8) gives the observed antenna temperature as a function of the distance x between the antenna axis and the limb of the moon. In this equation

$$(9) \qquad a = 1/0.6\,\Theta_E \qquad b = 1/0.6\,\Theta_H \qquad \Omega_m = \pi/ab = 1.133\,\Theta_E\,\Theta_H$$

and

$$(10) \qquad \eta_L'(\zeta') = \sqrt{2R\zeta' - \zeta'^2}; \qquad R \text{ is the moon's radius.}$$

The integration over η' yields $\frac{\sqrt{\pi}}{2b}\,\Phi\,[b\eta_L']$, where Φ means the error integral. This leads to

$$(11) \qquad T_A(x) = T_M \frac{(1-\beta_m)}{\Omega_m \cdot b}\sqrt{\pi}\int_0^{2R} \Phi[b\eta_L']\, e^{-a^2(\zeta'+x)^2}\, d\zeta'$$

This integral may be evaluated analytically only for the limiting case which neglects the curvature of the moon's limb. Then, $\eta_L' \longrightarrow \infty$ and $\Phi\,[b\eta_L'] = 1$ and equation (11) becomes

$$(12) \qquad \frac{T_A(x)}{T_M\,(1-\beta_m)} = \frac{1}{2}\,[1 - \Phi(ax)]$$

where the measured antenna has been normalized to the value $T_A(-\infty)$.

As an example we have evaluated equation (12) for a circular main beam and HPBW $5' \leq \Theta_A \leq 12'$, and the results are represented in Figure 8*. To get a rough experimental check of the calculation we take one of Hvatum's [2] drift curves over the moon measured at 8 GHz with the 85-foot antenna. At the time the measurement was made

---

* For the HPBW $5' \leq \Theta_A \leq 12'$, for which the curves in Figure 8 have been computed, one obtains identical results by assuming a square-shaped moon and normalizing the calculated curves to the antenna temperature at the center of this square.

(March 5, 1959, 1500 UT) the moon's age was 25.7 days. The measured drift curve shows a nearly perfect symmetry; so the center of the moon has been determined by drawing the line of symmetry. The time scale of the drift curve has been converted to an angular scale by considering the proper motion in RA, the declination and the parallactic motion in RA of the moon. In Figure 9 the measured antenna temperature, normalized to the value at the moon's center, has been plotted as a function of the angular distance from the moon's center. The dots correspond to the western part of the drift curve; the crosses correspond to the eastern part of the drift curve.

Now the fact that the measured drift curve does not attain zero values outside the moon's disk shows that the attenuation of the first sidelobes must have been very low. It cannot be expected, therefore, that the comparison of the computed drift curves (Fig. 8) with the measured drift curve (Fig. 9) leads to a very accurate value for the beamwidth. This is the reason that we only compared the linear parts of the theoretical and measured curves; the value of the HPBW obtained by this method is about 10'. If the measured and computed drift curves are normalized with the antenna temperature at the moon's limb, one obtains 8' for the HPBW of the antenna.

It is known that the true HPBW of the 85-foot antenna at this frequency was about 7'. There are two reasons that our method gives a larger value for the HPBW; we have neglected the influence of (a) the sidelobes and (b) the curvature of the moon's limb.

We feel that it should be possible to obtain valuable information about the antenna pattern at very high frequencies by refining this method. It seems to be worthwhile, therefore, to compute rigorous solutions to the convolution integral equation (11) by using the digital computer, and to consider in detail the influence of the first sidelobes.

References

[1] Mezger, P. G., Verzerrung radioastronomischer Beobachtungen durch Antennencharakteristik und Tiefpass. Zeitschrift fuer Instrumentenkunde, 66, H. 11, pp. 219-227 (1958).

[2] Hvatum, H., Private communication.

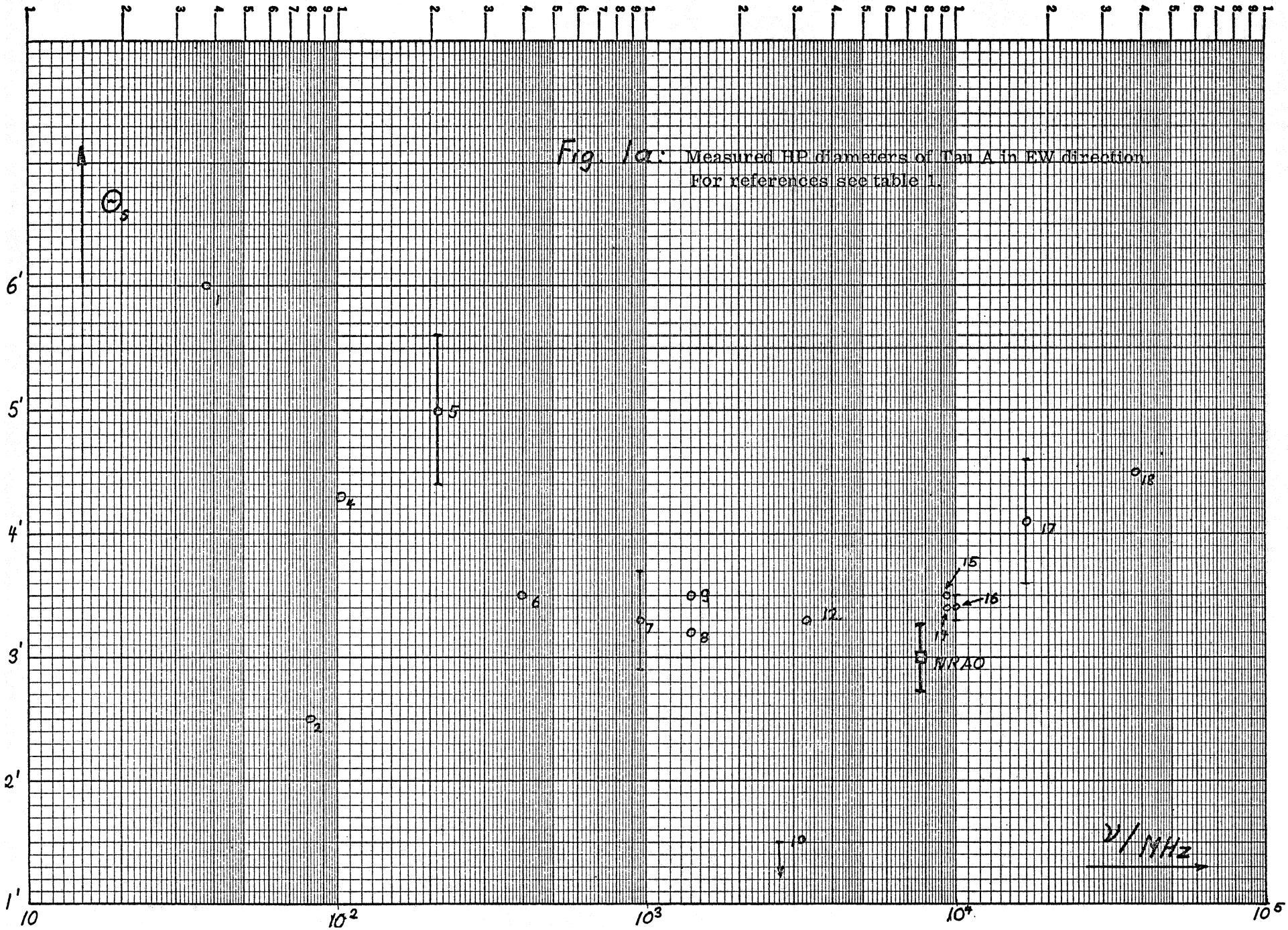

Fig. 1a: Measured HP diameters of Tau A in EW direction.
For references see table 1.

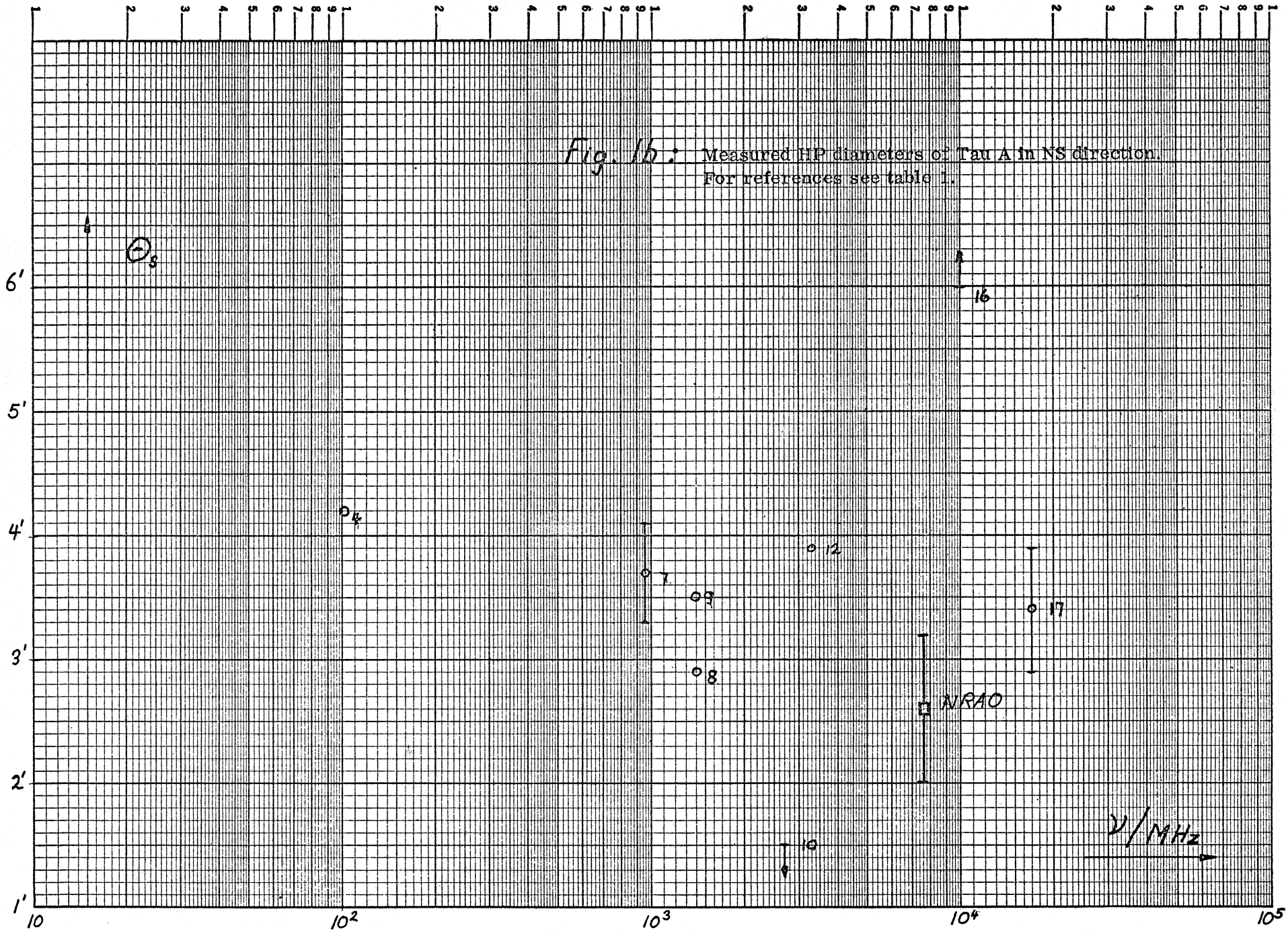

Fig. 16: Measured HP diameters of Tau A in NS direction.
For references see table 1.

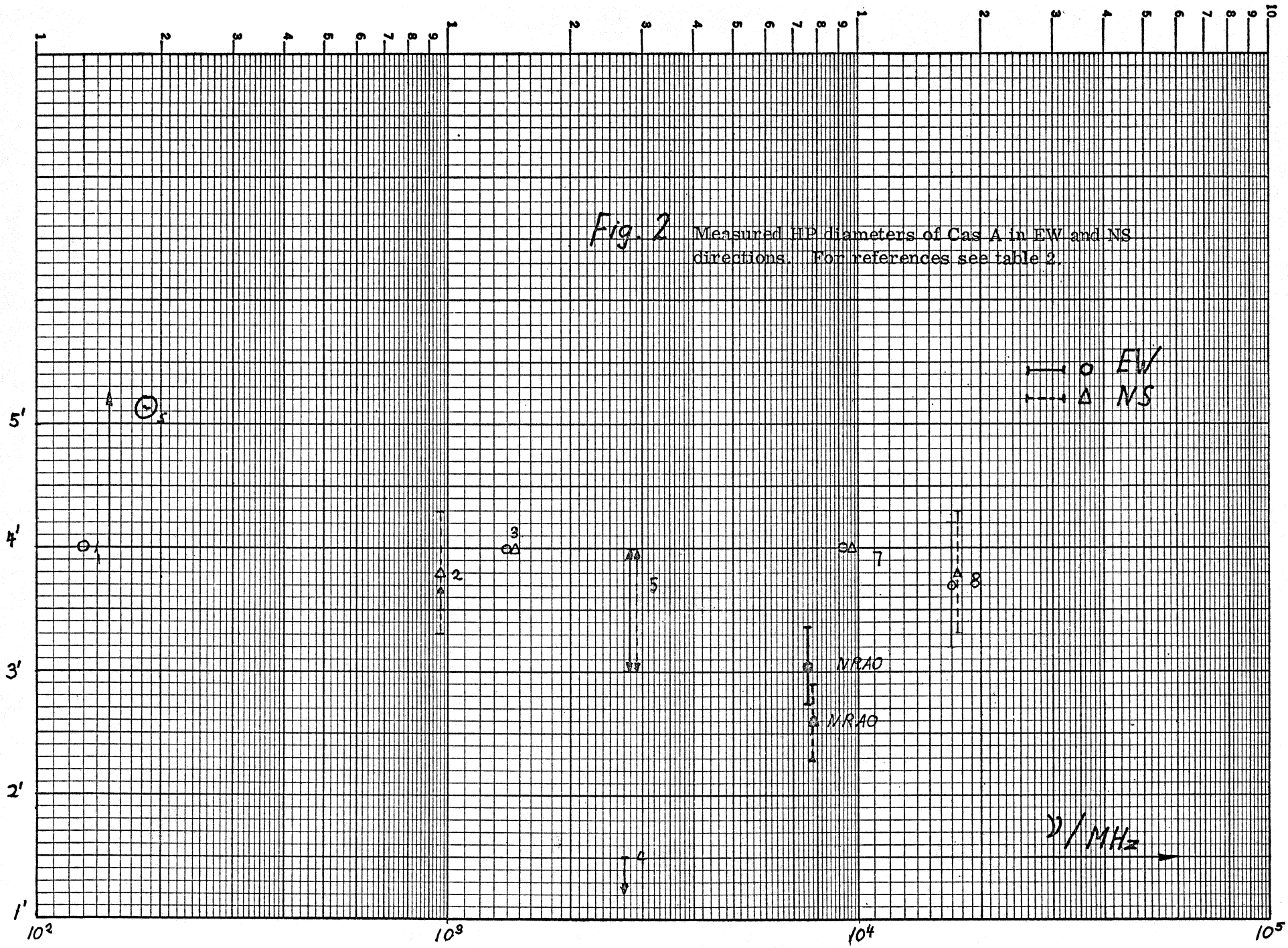

Fig. 2 Measured HP diameters of Cas A in EW and NS directions. For references see table 2.

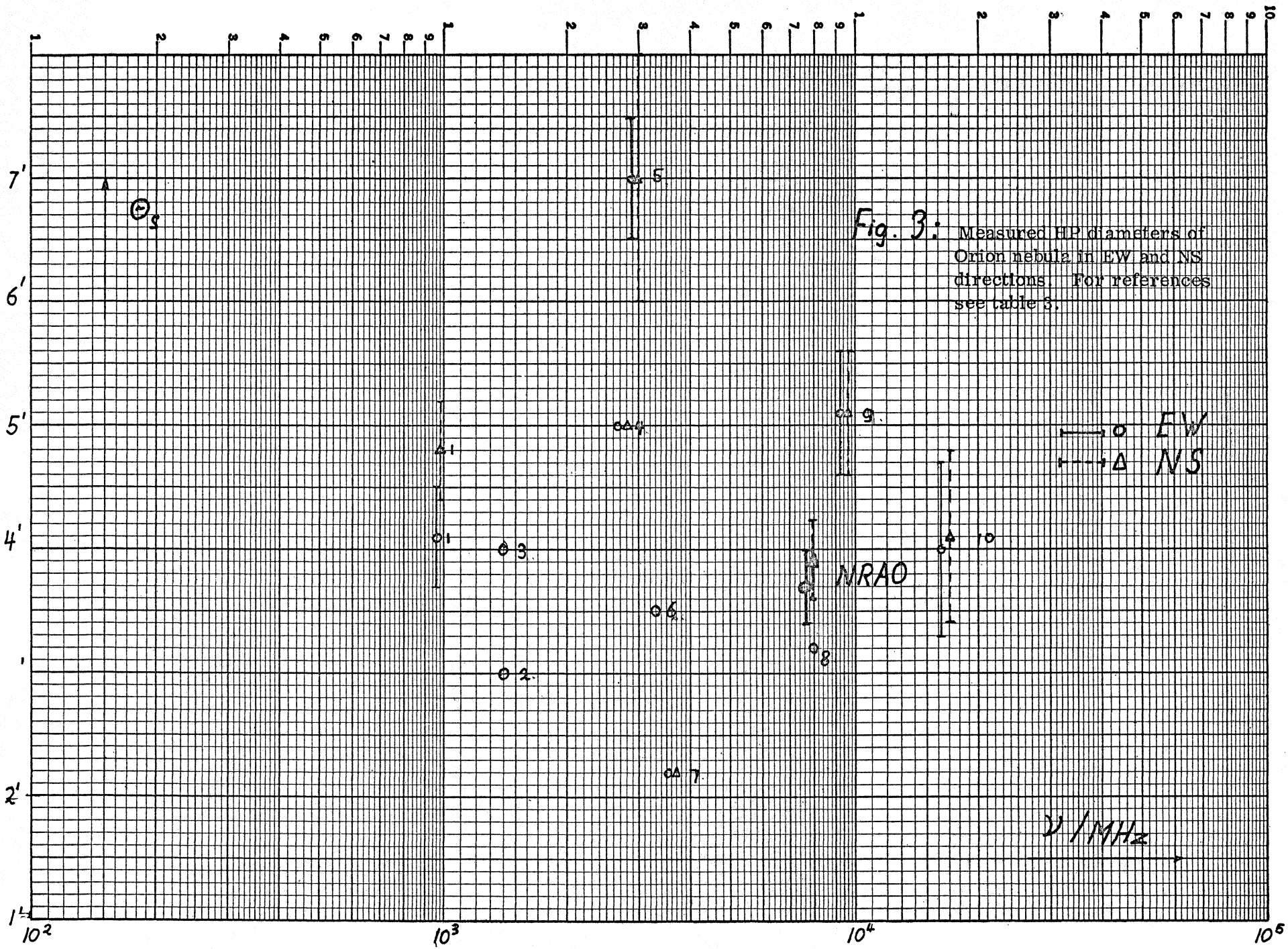

Fig. 3: Measured HP diameters of Orion nebula in EW and NS directions. For references see table 3.

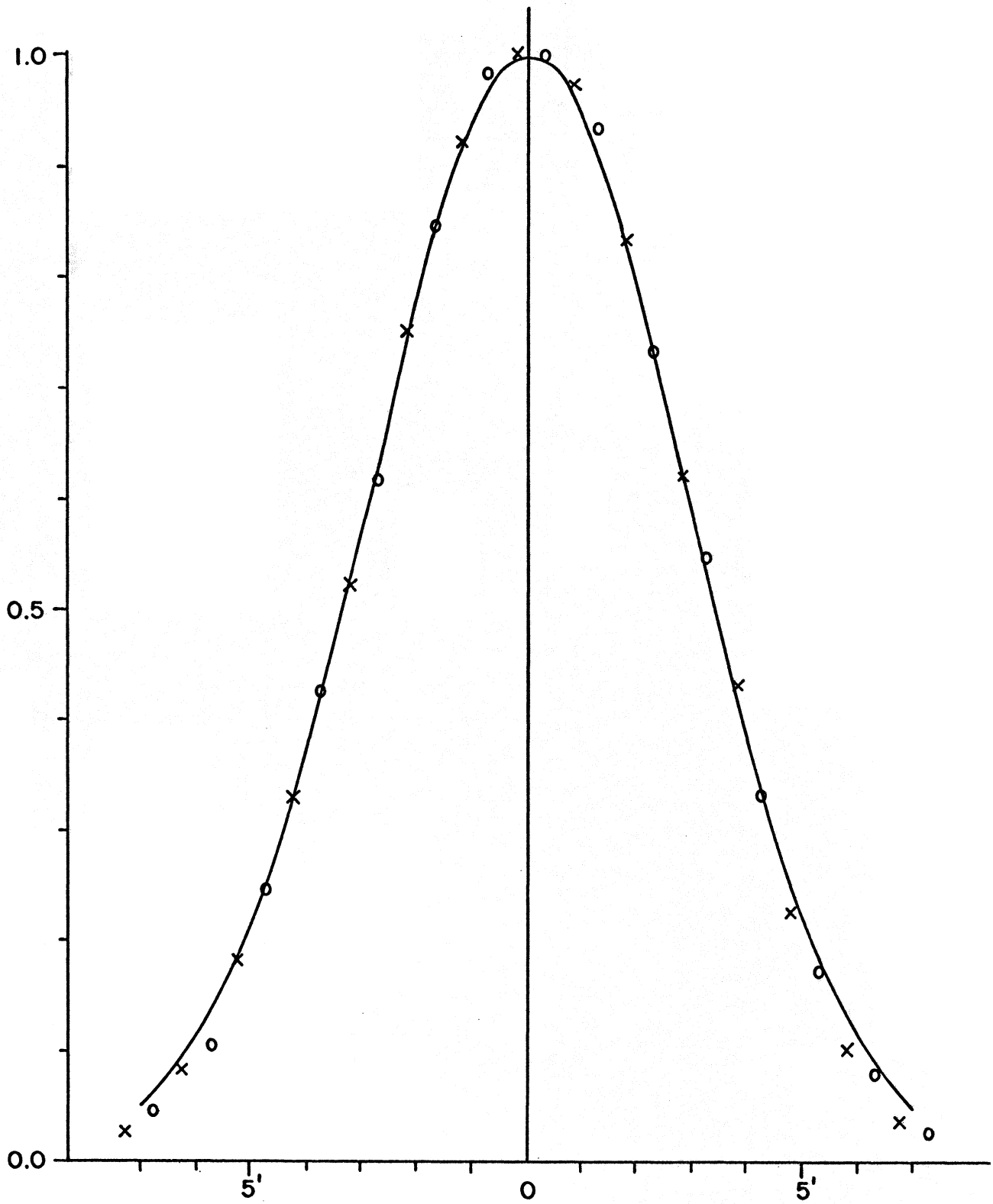

Figure 4. Normalized Cas A scan in declination, classified as "good" (7-22-63).
xx - scan south ($\Theta_A' = 6.80'$), oo - scan north ($\Theta_A' = 6.80'$).
HPBW adopted for the calculation of the gauss curve - $\Theta_\Delta' = 6.80'$.

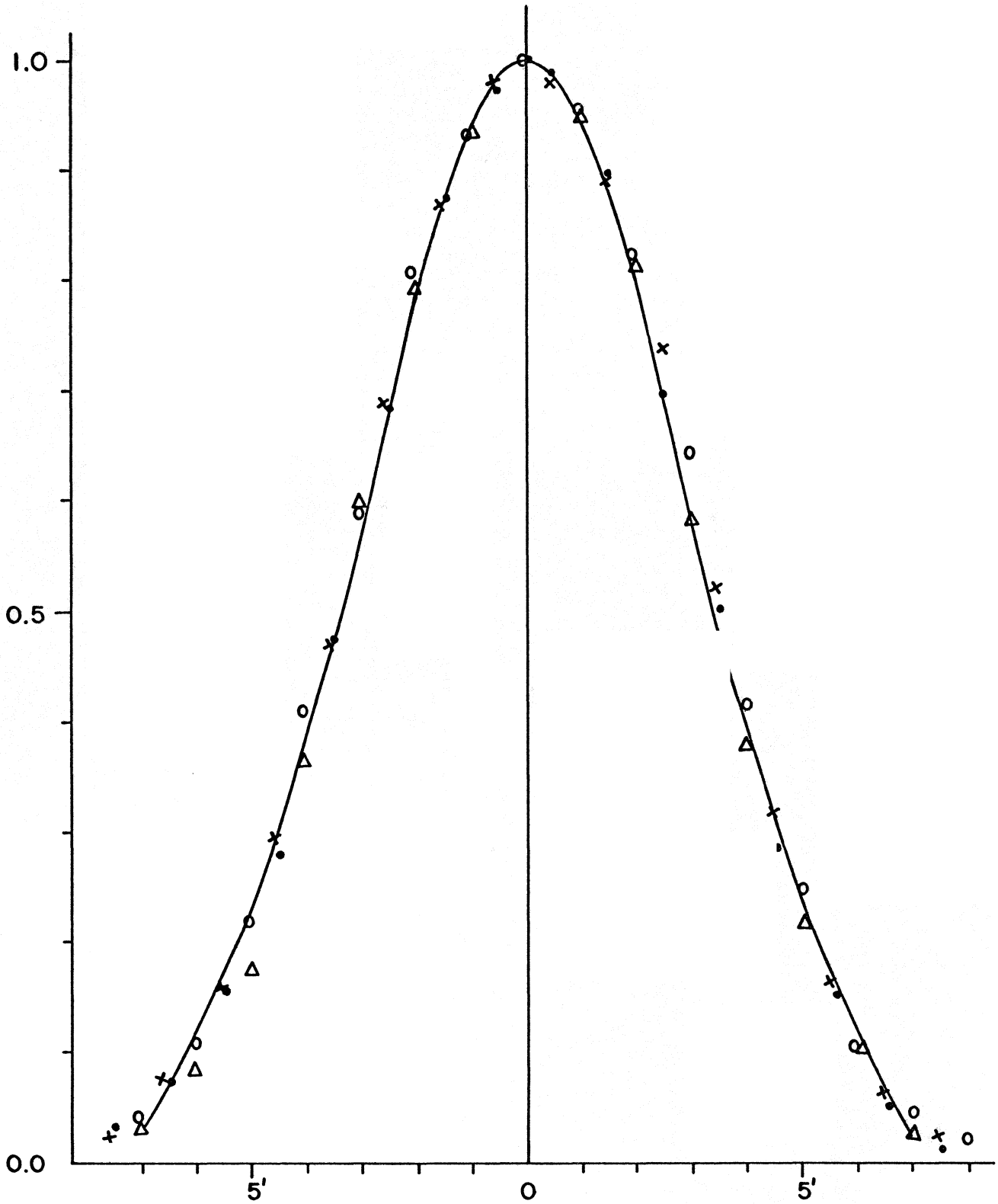

Figure 5. Normalized drift and scan curves of Cas A in RA, classified as "good" (7-22-63). xx - scan west ($\Theta_A' = 7.01'$), oo - drift east ($\Theta_A' = 7.16'$), .. - scan west ($\Theta_A = 6.9'$), $\Delta\Delta$ - drift east ($\Theta_A' = 6.85'$). HPBW adopted for the calculation of the gauss curve - $\Theta_A' = 6.95'$.

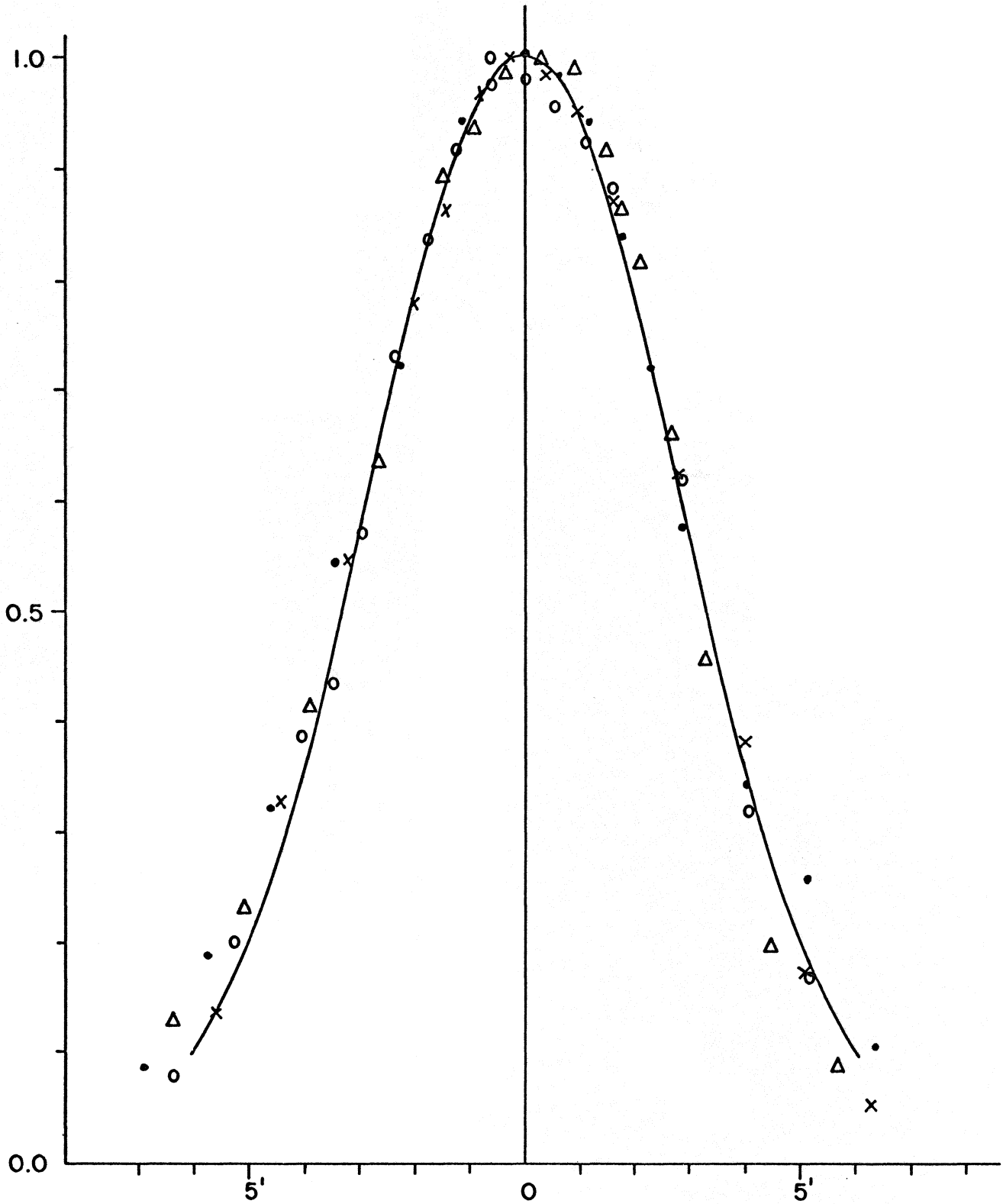

Figure 6. Normalized drift and scan curve of Cyg A in RA, classified as "bad" (7-21-63).
xx - scan west ($\Theta_A' = 6.8'$), oo - drift east ($\Theta_A' = 6.6'$),
$\Delta\Delta$ - scan west ($\Theta_A' = 6.6'$), .. - drift east ($\Theta_A' = 6.95'$)
HPBW adopted for the calculation of the gauss curve - $\Theta_A' = 6.60'$.

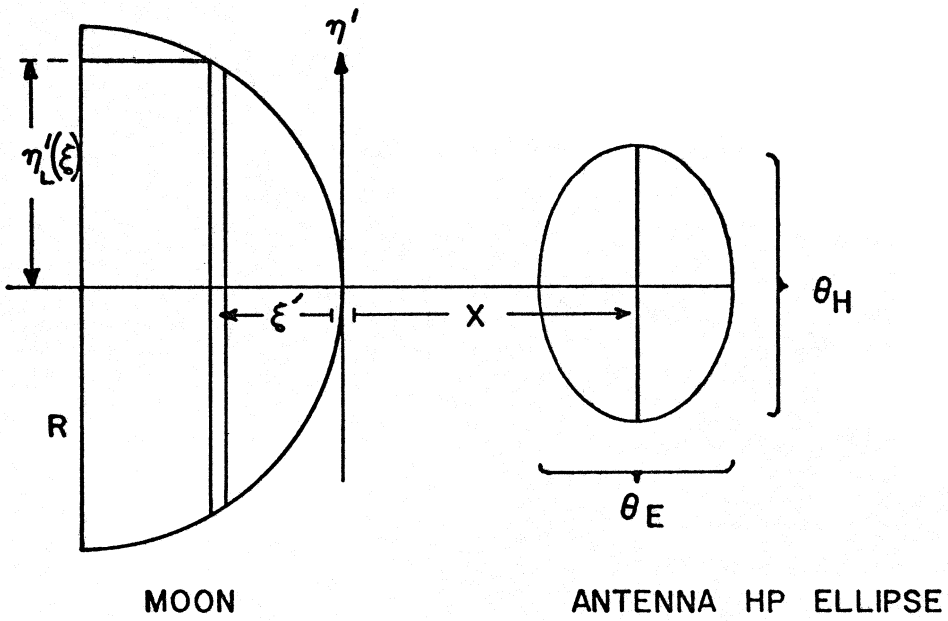

x = distance of the electrical axis of the antenna from the moon's limb.

ξ', η' = integration variables.

Figure 7. Geometry involved in the calculation of the convolution integral of antenna main beam and moon.

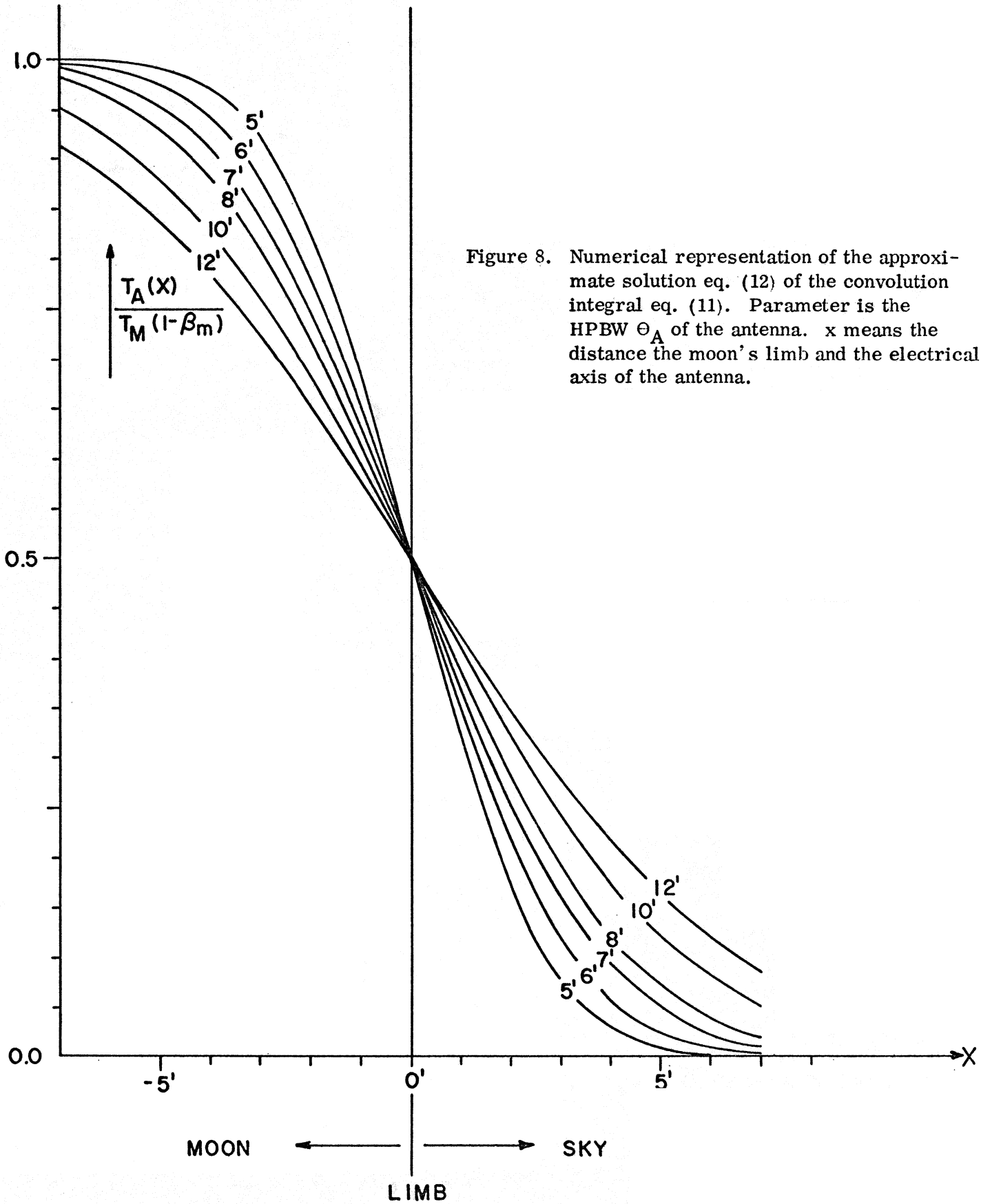

Figure 8. Numerical representation of the approximate solution eq. (12) of the convolution integral eq. (11). Parameter is the HPBW Θ_A of the antenna. x means the distance the moon's limb and the electrical axis of the antenna.

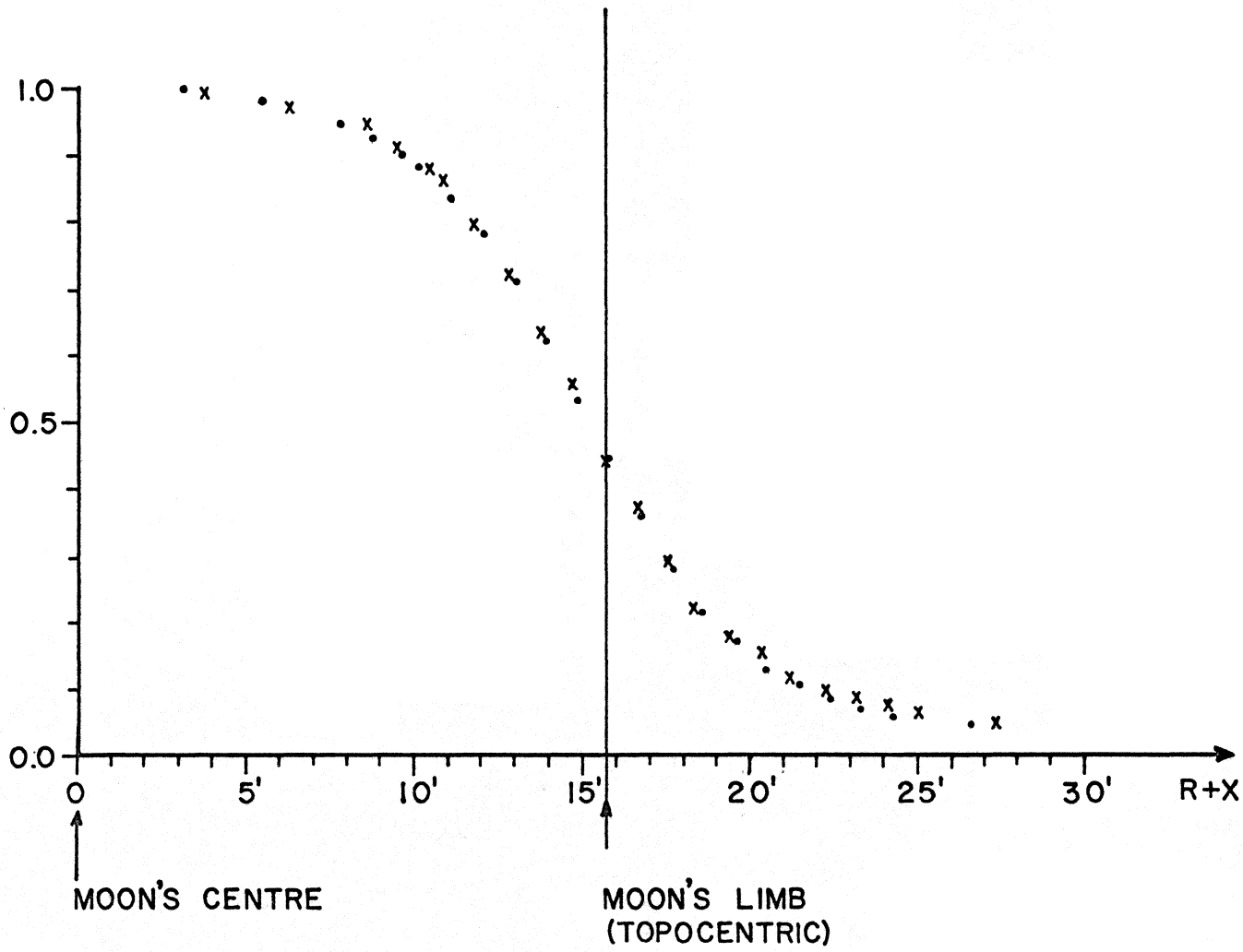

Figure 9. Normalized EW drift curve of the moon, measured by Hvatum (3-5-59) at 8 ± 0.25 GHz. R is the moon's radius, x is the distance between the moon's limb and the electrical axis of the antenna. .. - western part, xx - eastern part of the drift curve.